Paper No. 16

THE RELATIVE IMPORTANCE OF ACOUSTIC
SOURCES GENERATED BY HELICOPTER ROTORS
IN HIGH SPEED FLIGHT

S.E. WRIGHT

SCIENTIFIC ADVISER ONERA/AEROSPATIALE

September 20 - 22, 1976

Bückeburg, Federal Republic of Germany

THE RELATIVE IMPORTANCE OF ACOUSTIC

SOURCES GENERATED BY HELICOPTER ROTORS

IN HIGH SPEED FLIGHT

S.E. WRIGHT

SCIENTIFIC ADVISER ONERA/AEROSPATIALE

SUMMARY

A simple easy to use linear source theory is described. This theory represents most of the essential radiation properties of sources in arbitrary motion, including circular and helical motion appropriate to hover and forward flight. Possible sources of helicopter noise in high speed flight are then assessed, with particular reference to blade displacement, steady blade forces, unsteady blade forces and fluid stresses. It appears that unsteady blade forces are the most likely source of rotor noise, at least for present day forward flight speeds.

1.- INTRODUCTION

Just before the Second World War, Deming (1) (2) published his papers on the effect of blade thickness as a source of rotor noise. In these papers Deming implied that blade «thickness» noise was not an important source of rotor noise for rotors operating at reasonable levels of thrust, his exact words were : «The effect of thickness of blade sections of a propeller in producing noise is negligible except for very low angles of attack». Over forty years later, one finds references currently written on this subject, for example Lyon (3) Farassat (4) Hawkings and Lowson (5) have all argued recently that blade «thickness» noise is the dominant source of noise from high speed rotors. The author will now attempt to redress the balance in favour of A.F. Deming's original statement, at least for the present generation of rotorcraft. The main difficulty in establishing the truth, from a theoretical point of view, is the solution of the wave equation. For a complex source distribution such as that generated by a rotating blade system, and the further complication of the system advancing as a whole through space, makes the exact solution of the wave equation unattainable. Therefore, in order to obtain a closed form solution and to try and retain some physical understanding of the major radiation processes, the rotor disk in this paper is represented by a linear source array. Otherwise the blades are given the same kind of source properties as they would experience in circular motion. These linear source properties are then used to obtain estimates of the relative source strengths for each of the various kinds of rotor noise sources.

2.- RADIATION EQUATIONS

A theory dealing with acoustic source in linear motion has been described recently in reference (6), only the main steps in this theory and its applications are discussed here.

2.1.- Wave equation

The wave equation for the acoustic pressure P, resulting from acoustic disturbances in an otherwise inviscid and stationary propagating fluid, is well known, and can be written as :

$$\frac{1}{a_0^2} \frac{\partial^2 P}{\partial t^2} - \frac{\partial^2 P}{\partial x_i} = \frac{\partial^2 m}{\partial t^2} \text{ (or } \frac{\partial q}{\partial t}) - \frac{\partial f_i}{\partial x_i} + \frac{\partial t_{ij}}{\partial x_i \partial x_j} \tag{1}$$

where a_0 is the speed of sound in the surrounding fluid, and m, q, f_i, t_{ij}, are various types of input source strengths per unit volume (source densities), which can vary as a function of time or space over the source region. Physically, m can be interpreted for our purposes as the fluid mass per unit volume, displaced by a solid object moving through the propagating fluid i.e. $m = \rho_0 v$ where v is the volume displaced per unit volume, and ρ_0 is the density of the displaced fluid. The quantity of fluid or mass, per unit time per unit volume introduced or removed from the source region, is then $q = \pm \frac{\partial m}{\partial t}$. This latter source formulation is more appropriate to fluid injection sources such as jet effluxes.

The next order source, denoted by f_i, is illustrated in figure (1), it can either be interpreted as the double time derivative of fluid mass injection, and removal, times the separation distance d_i between the introduction and removal points ; or f_i can be considered as the applied force per unit volume required to produce this effect, i.e. $f_i = d_i \frac{\partial q}{\partial t}$. Similarly, the fluid stress source t_{ij}, also illustrated in figure (1), can be interpreted as two sets of fluid injection and removal points or two equivalent forces acting a distance d_j apart. Mathematically $t_{ij} = d_j f_i = d_i d_j \frac{\partial q}{\partial t}$, where the suffixes i and j signify the vector components

of position and magnitude along the three coordinate axis.

2.2.- Solution of wave equation

There are many possible solutions to the wave equation, as explained in reference (6). The solutions depend on the definition of the source distribution and disturbance functions. The distribution function describes how the source densities m, q, f_i, t_{ij} etc., vary locally across the source distributions, whereas the disturbance function gives information on how the source densities vary, as a whole, as a function of space or time. For instance it is possible for each point in the source distribution to vary together (inphase) as a function of time (time modulated source), or vary separately as a function of space, if the distribution is in motion (spatially modulated source). The source model assumed is for the spatially modulated case, here the source distributions are assumed to be moving through space, and experiencing a stationary disturbance with respect to a stationary propagating fluid. This type of source is considered to be more appropriate for aerodynamic disturbances generated by an aerofoil.

The solution of equation (1) also depends on the motion of the source distributions (flight path of each individual source). For arbitrary motion, there will be no simple closed form solution. However, if the source distributions are assumed to move in a straight line with constant velocity u, then there is a simple solution to the wave equation, given by equation (25) in reference (6) as :

$$(P_n)_{mB} = K_n \; \chi_s \; \chi_{mB} \; (\frac{\partial}{\partial t})^P \; [\, H \,] \qquad\qquad (2)$$

where n is the order of the source distribution based on the power of the space derivative, plus one, in equation (1) except $n = 0$. For example, a mass displacement source $n = 0$, a mass injection source $n = 1$, a force source $n = 2$, and a stress source $n = 3$, etc. The corresponding power of the time derivative p in equation (2) is unity for a mass injection and force source, and two for mass displacement and stress source radiation.

2.3.- Multipole order function

The multipole order radiation properties in equation (2) are contained in the K_n term. For a mass displacement, mass injection, force and stress source input, this term becomes :

$$K_0 = K_1 = \frac{1}{4\pi R} \qquad\qquad (3)$$

$$K_2 = \frac{1}{4\pi R a_0} \; \frac{X_i}{R} \qquad\qquad (4)$$

$$K_3 = \frac{1}{4\pi R a_0^2} \; \frac{X_i}{R} \; \frac{X_j}{R} \qquad\qquad (5)$$

R is the observer distance from the source region, and $\frac{X_i}{R}$, $\frac{X_j}{R}$ are the direction cosines the observer makes with the force and stress vectors respectively, as illustrated in Figure (1). These K terms have the directivities of a monopole, dipole and quadrupole source respectively, which are well known and therefore will not be considered further.

2.4.- Disturbance and distribution functions

χ_s and χ_{mB} are spectrum terms arising from the source disturbance and source distribution shape functions h_w and h_a respectively. These functions are harmonically analysed in the direction of motion, over the source region dimension d, as shown in figure (2). The amplitude of the disturbance function h_w corresponds to the integrated distribution source strength density summed across each source distribution of dimension a, thus :

$$h_w = \int_0^a h \; dx \qquad\qquad (6)$$

where h represents, generally, the various types of source strength densities m, q, f_i, and t_{ij}.

These density distribution functions are, of course, also equal to the sum of the individual density distribution functions, h_a, for each disturbance harmonic s, given by :

$$h = \sum_{s = 0}^{\infty} h_a \qquad (7)$$

The resulting spectrum functions in terms of s and mB, then become :

$$\chi_s = \frac{C_s}{2 (Avg)_w} \quad , \quad (Avg)_w = \frac{(area)_w}{d} \quad , \quad (Area)_w = \int_w |h_w| \, dx , \qquad (8)$$

$$\chi_{mB} = \frac{C_{mB}}{2 (Avg)_a} \quad , (Avg)_a = B \frac{(Area)_a}{d} \quad , \quad (Area)_a = \int_a |h_a| \, dx, \qquad (9)$$

where C_s and C_{mB} are the harmonic Fourier coefficients, $(Area)_a$ and $(Area)_w$ are the arithmetical areas enclosed by the corresponding shape functions and the x axis. mB is therefore a non dimensional radiation frequency term, where m is the sound pressure harmonic number, and B is the number of equispaced source distributions. The disturbance harmonic number s is then the non dimensional source frequency, and is related to the radiation frequency term by a Doppler shift given by :

$$s = \pm mB \, (M \cos \sigma - 1) \qquad (10)$$

$M = u/a_0$ is the Mach number of the source distributions, and σ is the angle the observer makes with the line of source motion. The plus and minus sign correspond to supersonic and subsonic source motions respectively.

2.5.- Retarded time function

The last term in equation (2), the retarded time source function [H], is from equation (23) ref. (6) :

$$[H] = H \cos (2 \pi f_r [t] - \theta_r) \qquad (11)$$

$$H = \frac{2(Avg)_a}{h_s} (Avg)_w \, d = 2 B (Avg)_w \qquad (12)$$

$$f_r = mBN, \quad N = u/d \qquad (13)$$

$$[t] = t - R/a_0 \qquad (14)$$

H is the total integrated source strength for the entire source region, which is basically the summation of the disturbance function, h_w, over the disturbance period w. h_s is the amplitude of the s spatial harmonic of the disturbance function, which is also equal to $(Area)_a$. The radiation frequency is given by $f_r = mBN$, where N is the distribution frequency (reciprocal of the time it takes for a source distribution to travel across the source region), and θ_r is the radiation phase angle with which we are not concerned here. [t] is the observer time or retarded time, which corresponds to the source time minus the time required for the radiation to reach the observer at a distance R from the source region. Finally the time derivative in equation (2) operates on the retarded time function giving :

$$(\frac{\partial}{\partial t})^p [H] = \pm H \, (mB2\pi N)^p \begin{matrix} \cos \\ \sin \end{matrix} (2\pi f_r [t] - \theta_r) \qquad (15)$$

The choice of polarity and function, sin or cos, depends on the order of the time derivative p.

3.- RECTANGULAR SHAPE FUNCTIONS

For real source distributions and disturbances, the χ_s and χ_{mB} spectrum functions are usually complicated, if is not complex. However, rectangular shape functions can be used to demonstrate the major radiation properties of actual shape functions, providing the arithmetical areas of the functions are made equal, as illustrated in figure (2). In this case, the spectrum functions given by equations (8) and (9) become,

$$\chi_s = \frac{\sin x}{x} \quad , \quad \frac{x = \pi s \rho_w}{s = \pm mB \, (M \cos \sigma - 1)}, \quad \rho_w = \frac{w}{d} \quad (Area)_w = A_w \, w \qquad (16)$$

$$\chi_{mB} = \frac{\sin x}{x} \quad , \quad x = \pi mB \rho_a \quad , \quad \rho_a = \frac{a}{d} \quad , \quad (Area)_a = A_a \, a \qquad (17)$$

where ρ_w and ρ_a are the disturbance and distribution solidities in terms of the source region size d, and where a, w, are the effective disturbance and distribution width respectively. Also the total integrated source strength, H, becomes, from equation (12)

$$H = 2B \, (Avg)_w = 2B \frac{(Area)_w}{d} = 2BA_w \, \rho_w \qquad (18)$$

where A_w, A_a are the amplitudes of the equivalent rectangular shape functions. It is these spectrum functions that give the major characteristic properties of sources in motion.

3.1.- Radiation spectrum

The spectrum properties of the disturbance and distribution functions are illustrated in figures 3 and 4. Figure 3 shows the construction of the spectrum from the three individual spectrum terms χ_s, χ_{mB} and $(mB)^p$, where the spectra are plotted in terms of mB numbers. The actual radiation spectra are found from mBN, where $N = u/d$ is the distribution frequency. The break frequencies in the mB spectra, (first frequency zeroes in the spectrum functions) are found by equating the arguments to π in the sin x/x functions, in equations (16) and (17) giving :

$$(mB)_w = \pm 1/ (M \cos \sigma - 1) \rho_w) \qquad (19)$$

$$(mB)_a = 1/ \rho_a \qquad (20)$$

It can be seen that the larger the disturbance and distribution solidities ρ_w, ρ_a, the lower the corresponding break frequencies and the lower the resulting high frequency radiation. The $\pm$ sign signifies supersonic and subsonic motion respectively. Note that the distribution mB spectrum is independent of source distribution speed, and that the disturbance spectrum is very sensitive to the source Mach number. The latter effect corresponds to the propagated disturbance sharpening in the direction of source motion ($\sigma = 0 \rightarrow 90°$) and lengthening to the rear ($\sigma = 90° \rightarrow 180°$). The gradient of the spectrum envelope above the break frequency of each of the individual disturbances and distributions spectrum functions, «rolls off» at 6dB per octave as shown in figure 3(a). The shape of the final composite spectrum therefore depends on the position of the two break frequencies $(mB)_w$, $(mB)_a$, and the power of the radiation frequency multiplier $(mB)^p$, given by equations (2) and (15). For a mass displacement and stress source distribution, $p = 2$, and the spectrum will have a 12 dB per octave uplift.. If the distributions are mass injection or force sources, then $p = 1$ and the spectrum will have a 6dB per octave uplift, as illustrated by the second figure in figure 3. Generally the source distribution size is smaller than the disturbance scale, making the distribution spectrum break frequency, occur at a higher frequency than the disturbance function break frequency; for simplicity, only the envelope of the spectrum functions are shown in the lower figure of figure (3).

3.2. Radiation directivity

The directivity is given as a product of the directivities of the disturbance function χ_s and the multipole order function K_n ; the χ_{mB} function is omnidirectional. At low source speeds, low frequencies (low mB numbers) and small disturbance solidities ρ_w, the χ_s directivity is almost symmetrical (non-directional), allowing the K_n directivity in figure (1) to become most apparent. At high speeds, the χ_s function becomes the dominant directivity, producing a fascinating acoustic beaming effect as illustrated in figure (4). For source speeds below Mach one, the radiation is most intense in the direction of motion. For supersonic source speeds, the maximum radiation $\chi_s = 1$, lies along the Mach wave angle, given by :

$$\cos \sigma = 1/_M \qquad (21)$$

The first directivity zero each side of the Mach wave angle, is given by equating the argument to π in equation (16) and rearranging thus :

$$\cos \sigma_w = \frac{1}{M} \quad (1 \pm \frac{1}{mB \, \rho_w}) \qquad (22)$$

The positive sign corresponds to the angle nearest to the direction of motion. For subsonic source speeds, only the negative sign applies, and the angle is then taken from the direction of motion. For a given frequency (mB number), the corresponding disturbance harmonic number s contributing to this frequency is also shown in figure (4).

3.3.- Steady disturbance

Of special interest, is the condition when the disturbances solidity ρ_w is unity. This situation corresponds to the motion of a steady disturbance across the source region, where the integrated source strength across each source distribution remains unchanged, (steady) during its entire passage across the source region. It can be seen in figure 3, that as the disturbance solidity increases, the spectrum break frequency reduces. When ρ_w is unity this break frequency is very low indeed,and the disturbance spectrum function then becomes from equation (16) :

$$\chi_s = \frac{\sin x}{x} \quad , \quad x = \pi \, mB \, (M \cos \sigma - 1) \qquad (23)$$

This function is important for steady disturbances in linear motion, such as steady aerodynamic forces and fluid mass displacements, generated by a moving rigid body. The spectrum and directivity properties of this function are, of course, those illustrated in figures (3) and (4) for $\rho_w = 1$.

3.4.- Comparison between linear and circular motion

The theory so far discussed has been concerned with rectilinear motion. However, these linear source properties can be used to indicate the major radiation characteristics of sources in circular motion. For disturbance length scales small compared with the source region size, ρ_W small, there is little difference between a linear source region, a region curved in a circular arc, or indeed a region joined to form a complete loop (annulus), as illustrated in figure (5). If ρ_W is zero then of course there is absolutely no difference between these source situations. As ρ_W increases, so do the differences in the radiation properties. The worst situation occurs for a steady disturbance $\rho_W = 1$. Here linear motion produces an acoustic beam in the direction of motion, whereas circular motion, produces as one would expect intuitively, a symmetrical directivity about the axis of rotation equivalent to rotating the acoustic beam through 360 degrees. From a radiation level point of view, the situation at subsonic speeds is crudely analogous to comparing a bar and ring magnet - the radiated flux is always highest in the open loop case. Also there are no interference zeroes, in the case of circular motion for subsonic source speeds.

The corresponding disturbance spectrum function for circular motion at constant velocity, to be compared with equation (23) is given by :

$$J_{mB} \ (x), \quad x = mBM \ \cos \sigma \qquad\qquad (24)$$

J is a Bessel function of order mB and argument (x). This function appears in the theories of Gutin (7) who first investigated, in depth, the radiation, from steady rotating blade forces. The function was also used later by Deming (1) in his theories on blade thickness. Now for an observer away, from the axis of rotation ($\sigma \neq 90$), equation (24) has the apparent properties of an accelerating source, that is the source appears to speed up and slow down as it advances and retreats away from the observer. Therefore, this function, not only, represents circular motion, but can, also be used to give the essential properties for forward flight (helical motion), providing the effective blade velocity in the direction of the observer is used.

4.- ASSESSMENT OF ROTOR NOISE

In order to assess the relative magnitudes of the various types of rotor noise sources, the linear source theory together with rectangular source disturbances and distribution functions is used. This linear source theory will in general represent the major radiation properties of a hovering rotor, and also forward flight effects providing the maximum resultant blade velocity, (usually the rotational plus forward speed) is used at the time of disturbance. For a more detailed comparison of the radiation, the disturbance and distribution shape functions will have to be defined in more detail, together with variation in effective blade speed. For transient disturbances, ρ_W small, the linear disturbance spectrum functions χ_s will adequately represent the radiation from circular and helical motion, however for steady disturbances, the steady disturbance spectrum function equation (23) is more accurately represented by the circular spectrum function J_{mB}, in equation (24). The distribution spectrum function χ_{mB} is independent of the blade trajectory. In the case of forward flight, there will be a Doppler shift in the spectrum in addition to that given by the linear source-stationary region theory. However for present day helicopter forward flight speeds (M < 0.3) this effect is neglected.

4.1.- Possible sources

There are three sources of noise that could contribute to high speed rotor noise, they are :

(1) Fluid displacement effects caused by blades of finite thickness

(2) Forces applied to the fluid generated by the aerodynamic lift and drag forces, and,

(3) Fluid stresses created in the fluid (blade boundary layer and wake) generated by viscosity effects.

In the absence of tip jets and other such types of fluid effusion, the mass injection source is ignored. Multipole sources of higher order than the quadrupole (stress source) are also neglected, as they appear to have no physical meaning in this particular application. Since high speed rotor noise is comprised of a series of impulses, giving rise to a discrete acoustic spectrum (rather than bursts of broadband noise), only steady and periodic variations in the various source strength densities are considered. Thus from equation (2), the discrete sound pressure spectrum from any multipole source distribution in constant rectilinear motion, is given as :

$$(P_n)_{mB} = K_n \ (\chi_s)_n \ (\chi_{mB})_n \ (\tfrac{\partial}{\partial t} \ )^p \ [H_n]$$

p = 1 for n = 1 and 2

p = 2 for n = 0 and 3

s = ± mB (M cos σ − 1) (spatially modulated source).

For the three sources listed above, the acoustic radiation becomes :

Fluid displacement (n = 0)

$$P_0 = K_0 \ (\chi_s)_0 (\chi_{mB})_0 \ (2 \pi f_r)^2 \ H_0 \qquad (25)$$

Applied force (n = 2)

$$P_2 = K_2 \ (\chi_s)_2 \ (\chi_{mB})_2 \ 2 \pi f_r \ H_2 \qquad (26)$$

Applied stress (n = 3)

$$P_3 = K_3 \ (\chi_s)_3 \ (\chi_{mB})_3 \ (2 \pi f_r)^2 \ H_3 \qquad (27)$$

The multipole acoustic properties of the K_n function are discussed in section 2.3 (equations (3) (4) and (5)). The disturbance and distribution spectrum characteristics χ_s, χ_{mB}, are described in sections 2.4 and 3 (equations (16) and (17) respectively) and the radiation frequency f_r is discussed in section 2.5 Only the total integrated source strengths, H, for the various types of sources need now be considered.

4.2.- Blade displacement source

Assuming that the constant spatial variations in fluid density, in which the blade rotates, are negligible, and that the physical volume of the blade does not change, then it is difficult to imagine how the fluid mass displaced by the rotating blade, can vary. The unsteady component of mass displacement is therefore neglected. From equations (18) and (6) the total integrated source strength for the steady component of displacement is given by :

$$H = 2BA_W \ \rho_W, \ A_W = h_W = \int_0^a hdx, \ h = m = \rho_0 v \qquad (28)$$

$$thus \ H_0^s = 2B \ \rho_0 \int_0^a v \ dx = 2B \ \rho_0 A_a \ a \qquad (29)$$

The super script, s, in equation (29) is used to indicate the steady component of displacement. ρ_W in equation (18) is unity for a steady disturbance, and the source strength density h for a displacement source becomes, $m = \rho_0 v$. A_a is the amplitude of rectangular distribution function, in this case it is the average chord thickness. ρ_0 is of course the density of the displaced fluid and B is the number of blades. The integral $\rho_0 \int v \ dx$ in equation (29) is the displaced fluid mass, per unit span of the blade,

as illustrated in figure (6). Using the chord thickness, c, for convenience instead of the average thickness A_a, the approximate source strength for the entire rotor of effective span length b is then :

$$H_0^s = 2B \ \rho_0 \ a \ b \ c \qquad (30)$$

where a b c is the effective volume of each rotor blade. If the rotor blades are travelling in a straight line, then the effective span length of the rotor would be its actual length. However for circular motion, each element along the span is travelling at a different speed, and therefore, an effective span length must be used. One possible estimate is to take b as being its actual length and then using an effective or acoustically average rotor speed of something like 0.8 of the tip speed. A second possibility is to take b as being about 20 % of the actual span, and assuming an effective speed of about 0.9 of the tip speed.

4.3.- Blade force source

The blade forces can and do vary as the blade rotates, therefore in this case, there will be acoustic radiation from both the steady and unsteady force terms. The total integrated source strength per unit span for the steady blade forces is from equation (18) and (6), where : $A_W = h_W = \int_0^a f_i \ dx$

and f_i is the force per unit area along the chord.

$$H_2^s = 2B \int_0^a f_i \ dx = 2B \ (A_a)_2^s \ a \qquad (31)$$

ρ_W is again unity in equation (18), and $(A_a)_2^s$ is now the mean level of the steady aerodynamic pressure distribution across the chord. The total integrated source strength of the entire rotor of span length b is then :

$$H_2^s = 2BL, \ L = \int_0^a \int_0^b f_i \ dx \ dy \qquad (32)$$

The double integral in the above equation, is the total load (force) developed by each blade of span length b as illustrated in figure 6 (b). In a similar fashion to the steady displacement source, b has an effective length, depending on how the source speed, in terms of the rotor tip speed, is defined. Unlike the displacement source, the multipole order function in this example, K_2, has directional properties, the directivity of which is given by the direction cosine term in equation (4). For the geometry given in figure 6 (b), equation (4) becomes :

$$K_2 = \frac{1}{4 \pi R a_0} \ \frac{x_i}{R} \ , \ \frac{x_i}{R} = \cos (\beta + (90 - \sigma)) = \sin (\sigma - \beta) \qquad (33)$$

where β is the effective force angle made with a parallel to the axis of rotation, and σ is the observation angle made with the direction of motion (plane of rotation).

Assuming that each blade has a similar loading time history, the total integrated source strength, from equation (18) for the unsteady component, is given by :

$$H^u_2 = 2 B \rho_w \, A_w = 2B \rho_w \, \Delta L \qquad (34)$$

where the super script u now signifies the unsteady component, and A_w is the usual integrated source strength per unit span (equation (6)). In the absence of detailed blade loading data, A_w can be taken as the total load (force) change per blade, ΔL, operating at an effective rotor radius of 0.9 of the rotor tip radius. Variations in blade loading can occur through flow distortions or forward flight asymmetry, in which case ρ_w will be large , or through small scale load disturbances (ρ_w small) generated for example by tip vortex-blade interactions, blade stall, drag divergence effects, etc.

4.4.- Fluid stress source

In the case of a rotor blade, the stress source is not so well defined as the two lower order sources just considered. However, the total integrated source strength is again given by equations (18) and (6) as :

$$H = 2 BA_w \rho_w, \quad A_w = h_w = \int_0^a h \, dx \, , \, h = t_{ij} = d_j \, f_i \qquad (35)$$

$$\text{giving}: H_3 = 2B \rho_w \int_0^a d_j \, f_i \, dx \qquad (36)$$

Little is known about the disturbance scale (ρ_w), the magnitude of the stress forces f_i and the separation distance d_j between their effective points of application. Also details regarding the effective source length scale, (a), are not clear. It is conceivable that f_i, which is presumably proportional to the drag forces, is of an order of magnitude less than the steady aerodynamic forces on the rotor. d_j is taken as some dimension of the order of the boundary layer thickness, say a/1000, and the effective a, is some dimension smaller than the chord dimension.   In this case, the stress source strength density $t_{ij} = d_j \, f_i$ will be less than 10^{-4} of the steady aerodynamic force strength density (equation (31)). Further, comparing the multipole order function, K_n for the force and stress source, given by equations (4) and (5), it can be seen that the stress source term is smaller than the force source term by a factor of the speed of sound, a_0. This reduction will be exceeded by a factor of two, at the frequencies of interest (100 Hz), by the difference in power of the radiation frequency $2\pi f_r$, between the two equations (26) and (27). Thus the stress source radiation will be at least three orders of magnitude (60 dB) less than the force source intensity for the steady component, and something greater than this for the unsteady stress component. The stress source will not be considered further at this time.

4.5.- Comparison between steady displacement and force sources

Of particular interest is the relative levels of acoustic radiation generated by the displaced fluid, and aerodynamic forces developed by the rotating blades. From equations (25) and (26) and using J_{mB} rather than χ^s_s, the ratio of the acoustic pressures for the steady displacement and force source, can be written as :

$$\frac{P^s_0}{P^s_2} = \frac{K_0}{K_2} \, \frac{(J_{mB})_0}{(J_{mB})_2} \, \frac{(\chi^s_{mB})_0}{(\chi^s_{mB})_2} \, \frac{H^s_0}{H^s_2} \, 2\pi f_r \qquad (37)$$

If one assumes a rectangular chord distribution of similar length scale for both the blade thickness, and steady force distribution, then the break frequencies given by equation (20) will take effect in the same region of the high frequency spectrum, making $(\chi^s_{mB})_0 \simeq (\chi^s_{mB})_2$. This equality is particularly true at low frequencies, where each function approaches unity value. Also, the displacement and force spectrum functions are exactly the same providing one assumes the same effective blade speed for each type of source. Therefore, it makes no difference whether one uses $(\chi^s_s)_0 = (\chi^s_s)_2$, $(J_{mB})_0 = (J_{mB})_2$

or some other function. The ratio of the sound pressures in equation (37) can therefore be written as :

$$\frac{P^s_0}{P^s_2} = \frac{K_0}{K_2} \, \frac{H^s_0}{H_2} \, 2\pi f_r \qquad (38)$$

Subsituting for the multipole order functions, K_0, K_2, given by equations (3) (33) and the total source strengths H^s_0, H^s_2, described by equations (30)(32); equation (37) reduces to :

$$\frac{P^s_0}{P^s_2} = \frac{a_0}{\text{Sin}\,(\sigma - \beta)} \, \frac{\rho_0 \, abc}{L} \, 2\pi f_r \qquad (39)$$

$$\text{or } f_r = \frac{L}{\rho_0 \, abc} \, \frac{\text{Sin}\,(\sigma - \beta)}{2\pi a_0} \quad \text{when } P^s_0 = P^s_2 \qquad (40)$$

$$\text{where} \quad \frac{L}{\rho_0 \, abc} = \frac{C_L}{2c} \, V^2_e$$

ρ_0 abc is the displaced mass of fluid per blade and L is the laod per blade in Newtons. C_L is the lift coefficient, and V_e is the effective rotor speed taken to be at 0.9 of the tips radius. The load per unit displaced mass, L/ρ_0 abc , for a rotor developing a reasonable thrust, is at least 100,000, if b is taken to be complete span length. However as the load is heavily weighted toward the blade tip, and the blade thickness is roughly constant along the span, then the effective b is only about 20 % of the tip radius. Also for an observer situated in the general direction of the load vector, sin $(\sigma - \beta)$ is approximatly unity when expressed in logarithmic units. Therefore, taking account of the speed of sound a_0, the radiation from the steady blade forces is at least two hundred and fifty times (50 dB) more than that from the blade displacement effect, at unity frequency. Thus for a given operational thrust, and all observation angles except those close to the normal to the thrust vector, the blade displacement radiation can never equal the radiation from the steady blade forces at low frequencies — irrespective of rotor speed.

Now, because the displacement radiation increases at a rate of 12 dB per octave in comparison with 6 dB per octave for the force source (the difference in power of the frequency term in equations (25) and (26)), the displacement radiation will potentially exceed that of the force source at some frequency in the region of 250 Hz, (mB = 50 if N $\approx$ 5 Hz, as given by equation (40) and depicted in figure 7 (a)). However the overiding condition as to whether this high frequency radiation will in fact radiate, depends on the value of the spectrum function J_{mB}, which is of course, a function of rotor speed. For a high forward speed rotor with an advancing tip Mach number of say 0.9 (effective speed 0.8), J_{mB} is rapidly reducing at high frequencies, and is well cut off by the time it reaches mB = 50. Therefore the spectrum at these frequencies, from either the blade displacement or steady forces, is of little practical importance as illustrated in figure (7 (b)). At lower frequencies, the force term is very much the dominant source.

4.6.- Comparison between steady and unsteady force sources

As it appears that the blade forces are usually the dominant sources, at least for high performance subsonic tip speed rotors, it is now important to try and assess the relative magnitudes of noise generated by the steady and unsteady force components. From equation (26), and again using J_{mB} rather than χ^s_s, the ratio of unsteady to steady force source radiation is given by :

$$\frac{P^u_2}{P^s_2} = \frac{\chi^u_s}{J_{mB}} \frac{\chi^u_{mB}}{\chi^s_{mB}} \frac{H^u_2}{H^s_2} \tag{41}$$

One can again assume that the chord distribution spectrum functions for both the unsteady and steady forces are equal, ($\chi^u_{mB} = \chi^s_{mB}$). However, it should be pointed out that at high tip speeds, and short distances, there will be an increasing difference between these distribution functions. For a characteristic length of something like the chord dimension i.e. $\rho_a \approx 1$ %, differences in the χ_{mB} functions can be expected to occur around the break frequency of mB = 100, given by equation (20). However for frequencies below mB = 100, equation (41) can be adequately represent by :

$$\frac{P^u_2}{P^s_2} = \frac{\chi^u_s}{J_{mB}} \frac{H^u_2}{H^s_2} \tag{42}$$

Thus the relative level of acoustic radiation now depends only on the ratio of the disturbance spectrum funtions χ^u_s / J_{mB} and on the ratio of the total integrated source strengths H^u_2 / H^s_2 . Substituting for the integrated source strengths (equations (34) and (32)) where A_w has been replaced by the total integrated load change ΔL, the above equation becomes :

$$\frac{P^u_2}{P^s_2} = \frac{\chi^u_s}{J_{mB}} \frac{\Delta L}{L} \rho_w \tag{43}$$

$\Delta L/L$ is the fractional change in steady loading for a given disturbance solidity ρ_w. For convenience, the two spectrum functions χ^u_s and J_{mB}, are plotted in figure (8) in logaritchmic units as a function of frequency (mB) and for several effective resolved rotor speeds ($M_e \cos \sigma$). The χ^u_s function envelope, open curve, is given for a disturbance solidity ρ_w of 10 %, using a rectangular disturbance function. For sharper disturbances (lower solidities), the spectrum break frequency (mB)$_w$, given by equation (19), moves to the right as in the case of increasing tip speed. The main point concerning figure (8) is that the J_{mB} function (steady force radiation) is in general of a considerably lower value than the χ^u_s function (unsteady force radiation), particularly at low rotor speeds and small disturbance solidities.

More subtly, it can be argued that as $M_e \cos \sigma$ increases, the difference in level between χ_s^{u} and J_{mB} decreases, for a given ρ_w. Also the product $\chi_s^{u} \, \mu_w$ is independent of ρ_w above the break frequency $(mB)_w$. Therefore as the rotor tip speed increases, so must the relative magnitude of the unsteady forces $\Delta L/L$ to maintain the unsteady force dominance - irrespective of the disturbance duration (ρ_w). The effect of the disturbance solidity therefore serves only to modify the low frequency content through changing the disturbance break frequency - longer disturbances resulting in lower frequency content. The amplitude of the disturbance required to equal the steady force radiation at a particular frequency (mB), is from equation (43)

$$\frac{\Delta L}{L} = \frac{J_{mB}}{\chi_s^{u}} \frac{1}{\rho_w} \tag{44}$$

For example, at an effective advancing tip Mach number of $M_e = 0.8$, a frequency of 100 Hz $(mB = 20$ if $N \simeq 5$ Hz), and a disturbance solidity of $\rho_w = 10$ %, J_{mB} / χ_s^{u}, is approximately 1/100 $(-40$ dB), and the value of $\Delta L/L$ required to give an equal radiation level at $mB = 20$ is therefore $\simeq 10$ %. If now the disturbance solidity is increased to say 50 %, the decrease in χ_s^{u}, due to the function moving to the left, is offset by the increase in ρ_w, thus the level of $\Delta L/L$, necessary to maintain the radiation at $mB = 20$, is the same. This is an example of the remarkable fact that the peak radiation level of the resulting spectrum for a rectangular disturbance, is independent of the sharpness of the disturbance producing it.

4.7.- Comparison between steady displacement and unsteady forces

Finally, the ratio of the acoustic radiation from the unsteady blade forces and the steady displacement effect, is from equations (25),(26)

$$\frac{P_2^{u}}{P_0^{s}} = \frac{K_2}{K_0} \frac{(\chi_s^{u})_2}{J_{mB}} \frac{(\chi_{mB}^{u})_2}{(\chi_{mB}^{s})_0} \frac{2\pi f_r}{(2\pi f_r)^2} \frac{H_2}{H_2} \tag{45}$$

Substituting for the multipole order term K_n, the integrated source strengths H_n, and, assuming at low frequencies $(\chi_{mB}^{u})_2 \simeq (\chi_{mB}^{s})_0$, the above equation becomes :

$$\frac{P_2^{u}}{P_0^{s}} = \frac{\sin(\sigma - \beta)}{a_0 \; 2\pi f_r} \frac{\chi_s^{u}}{J_{mB}} \frac{\rho_w}{\rho_0 abc} \frac{L}{L} \frac{\Delta L}{L} \tag{46}$$

For radiation frequencies in the region of 100 Hz $(mB = 20$ if $N = 5)$, a tip speed of say $M = 0.9$ $(M_e = 0.8)$, and a disturbance solidity ρ_w of 10 %, $\chi_s^{u} \rho_w / J_{mB} \simeq 6$ $(15$ dB).For radiation away from the normal to the force vector $\sin(\sigma - \beta)/a_0 \; 2\pi f_r$ is approximately 1/200,000 $(-106$dB$)$, and again $L/\rho_0 \, abc$ is about 500,000 $(115$ dB$)$. Thus the ratio of the fluctuation forces compared with the steady forces, $\Delta L/L$ required to dominate the steady displacement radiation is about 1/15 or $(-24$ dB$)$.

4.8.- Measured data

Figure (9) is offered as experimental evidence to support the hypothesis that unsteady blade loading can in-fact dominate all other sources of rotor noise in high speed flight. Figure 9 (a) is included to show typical azimuthal variations in blade loading that can be expected at about 0.9 of the tip radius from a helicopter rotor at high forward speeds ; see for example, M. Tran Cam Thuy and J. Renaud in reference (8). The derivative of the blade loading is also shown as a function of azimuth angle. The point of interest is the large negatively going load change $(\Delta L/L \simeq -1)$ which coincides with the maximum advancing blade speed, $(\theta = 90°)$ giving a sinusoidal load derivative. According to the forgoing theory, this unsteady loading is more than enough to dominate any other rotor noise source. •

In an attempt to provide acoustical data of high speed flight, a Puma helicopter SA 330 was flown in a shallow descent over a stationary microphone. The pilot's instruments showed an air speed of $V_f = 150$ knots $(77$ m/s$)$ at an altitude of 30 metres. The rotational tip speed of the Puma was $V_r = 208$ m/s giving an advancing tip speed $V_r + V_f = 285$ m/s $(M_{r+t} = 0.84)$. Figures 9 (b) and (c) show the time history and integral of the time history for two horizontal separation distances from the microphone, as indicated in the approach and flyover «herring bone» signature shown at the top of the figure. Figure 9 (c) shows mes-surements taken when the helicopter was overhead, making $\sigma = 90°$. As the Doppler effect is negligible in this overhead position, the steady source terms such as blade displacement and steady blade forces give ne-gligible radiation, $(M_e \cos \sigma \simeq 0)$. Therefore, the acoustic signature here should simply be the summation

derivatives of the blade loading signatures. Conversely the integral of the acoustic signal, should give information regarding the time variation of the blade loading as the blade rotates. Bearing in mind that the SA 330 has 4 blades, the acoustic signature and integral will be a summation from four blades. Assuming that the acoustic signal is basically a sinusoidal variation over 180° of the rotor disk,and there is a 90° phase shift in the acoustic signal between each blade, a four bladed system should give acoustic cancellation in the overhead region (maximum flyover level). The signal does infact show a four times repetition of the residual radiation from the most dominant sinusoidal variation of the blade cycle. Figure 9 (b) appears to confirm this unsteady loading effect. At large distances from the microphone, $R \simeq 100$ m, $\sigma \longrightarrow 0$, the Doppler effect is at its strongest, and the signal from the highest speed part of the blade cycle has become compressed, thus revealing the individual signal from each blade. The acoustic integral and signature is now almost identical with typical blade loading and derivative shown in figure 9(a). Thus an impulsive acoustic signal results from what is basically a negative going blade loading disturbance, occupying about 50 % of the rotor circumference Another 4 bladed rotor, Dauphin SA 365, flying at a similar advancing tip speed, showed almost identical acoustic signatures to that of the Puma. Therefore, it is tempting to assume that the acoustic characteristics shown in figure (9) are typical of four bladed main rotor helicopters flying at high speed.

ACKNOWLEDGMENT :

REFERENCES

1.- A.F. DEMING — 1937 NACA TN 605 - Noise from propellers with symmetrical sections at zero blade angle.

2.- A.F. DEMING — 1938 NACA TN 679 - Noise from propellers with symmetrical sections at zero blade angle, II.

3.- R.H. LYON — 1971 J. of the Acoustical Society of America, 49.894-905. Radiation of sound by airfoils that accelerate near the speed of sound.

4.- F. FARASSAT — 1974, J. of Sound and Vibration, 32, 3, 387-405. The acoustic far field of rigid bodies in arbitrary motion.

5.- D.L. HAWKINGS and M.V. LOWSON, 1975, AIAA 2nd Aero-Acoustic conference 75-450. Noise of high speed rotors.

6.- S.E. WRIGHT 1976, Inst. of Sound and Vibration Research, Tech. Report No 68. Finite source distributions in motion.

7.- L. GUTIN 1936, Physikalische Zeilschrift der Sowjetunion Vol. 9, No 1, 57-71, also 1942, Zhural Teknichneskoi Fiziki 6, 899, 909, English translation 1947, NACA Tech. Memo No 1195. On the sound field of a rotating propeller.

8.- M. TRAN CAM THUY and J. RENAUD, 1975 - First European Rotorcraft and Powered lift Aircraft Forum University of Southampton. Evaluation théorique des phénomènes aérodynamique et dynamique sur un rotor en vol d'avancement.
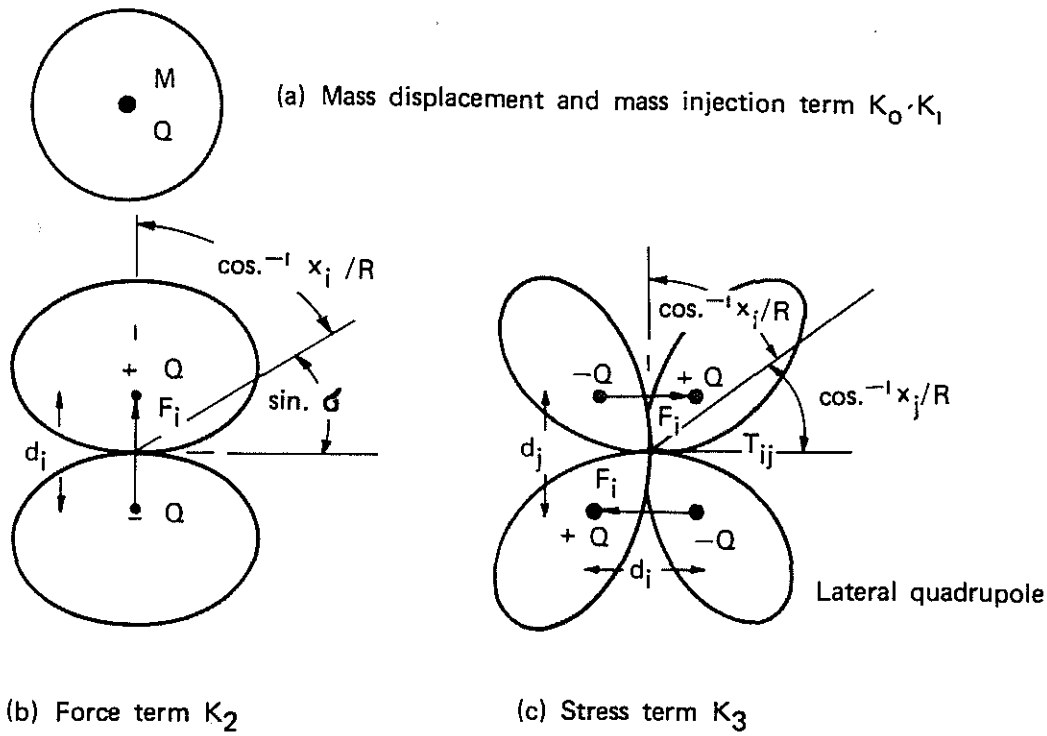
(a) Mass displacement and mass injection term $K_0 \cdot K_1$

(b) Force term K_2

(c) Stress term K_3

Fig. 1- DIRECTIVITIES OF THE K_n FUNCTION
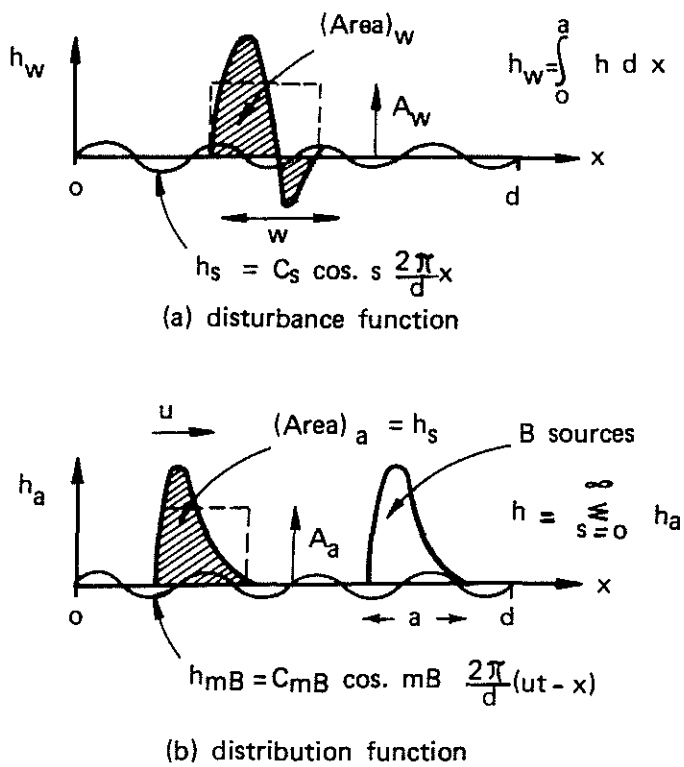
$h_w = \int_0^a h \, dx$

$h_s = C_s \cos. s \frac{2\pi}{d} x$

(a) disturbance function

$(Area)_a = h_s$

B sources

$h = \sum_{s=0}^{\infty} h_a$

$h_{mB} = C_{mB} \cos. mB \frac{2\pi}{d}(ut - x)$

(b) distribution function

Fig. 2 SOURCE DISTURBANCE AND DISTRIBUTION FUNCTIONS

(a) individual spectra

$(mB)a = 1/\beta a$

$(mB)_W = 1/\left((M\cos.\sigma - 1)\beta_W\right)$

10 dB

6 dB/2

$1/\pi\beta$

log (mB)

(b) complete spectrum

$(mB)^P$

$(mB)_e = 1/\beta a$

$(mB)_W = 1/\left((M\cos.\sigma - 1)\beta_W\right)$

log.(mB)

Fig. 3 - DISTURBANCE AND DISTRIBUTION SPECTRUM FUNCTIONS

$s = mB$

$X_s = 1$

$\cos.\sigma = 1/M$

$s = mB\ (M+1)$

$s = \pm mB(M-1)$

$\cos.\sigma_W = -\frac{1}{M}\ (1\pm\frac{1}{mB\beta_W})$

$s = mB$
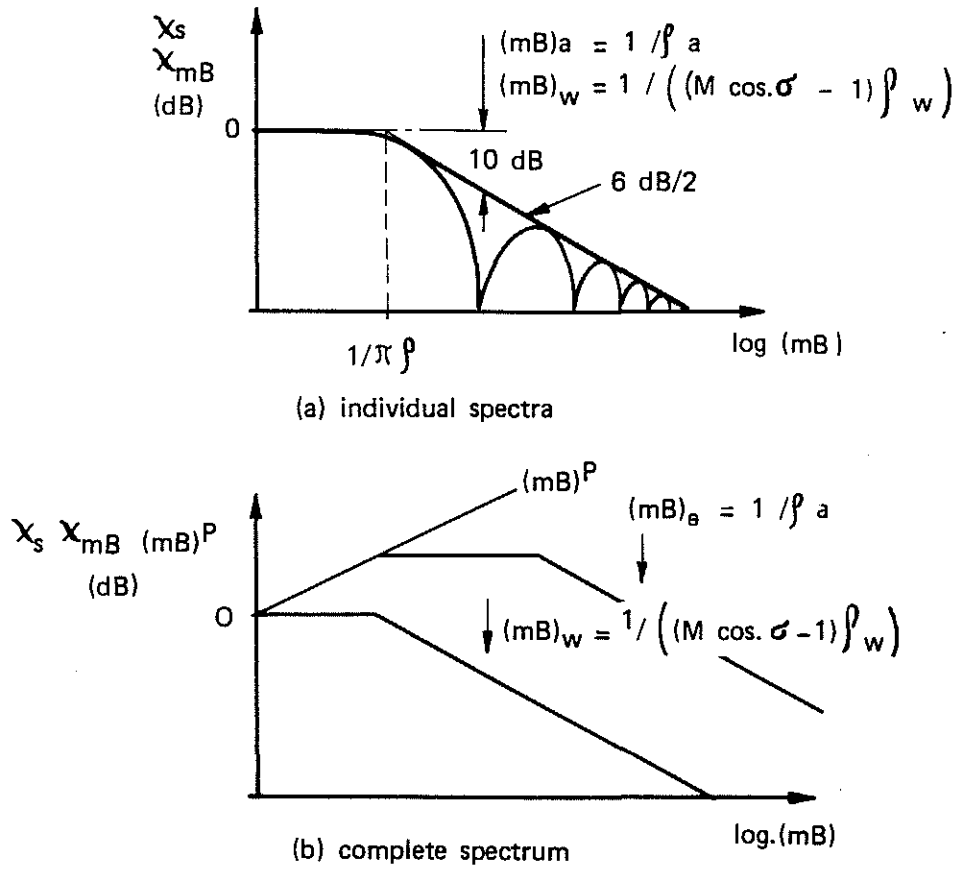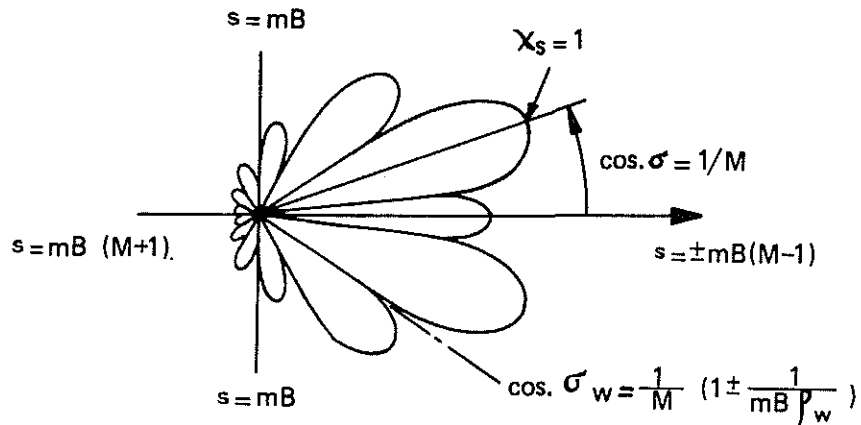
Fig. 4 - DIRECTIVITY OF DISTURBANCE SPECTRUM FUNCTION X_s

Linear

Circular

(a) $\int_W$ small (w≪d)

(b) $\int_W$ unity (w=d)
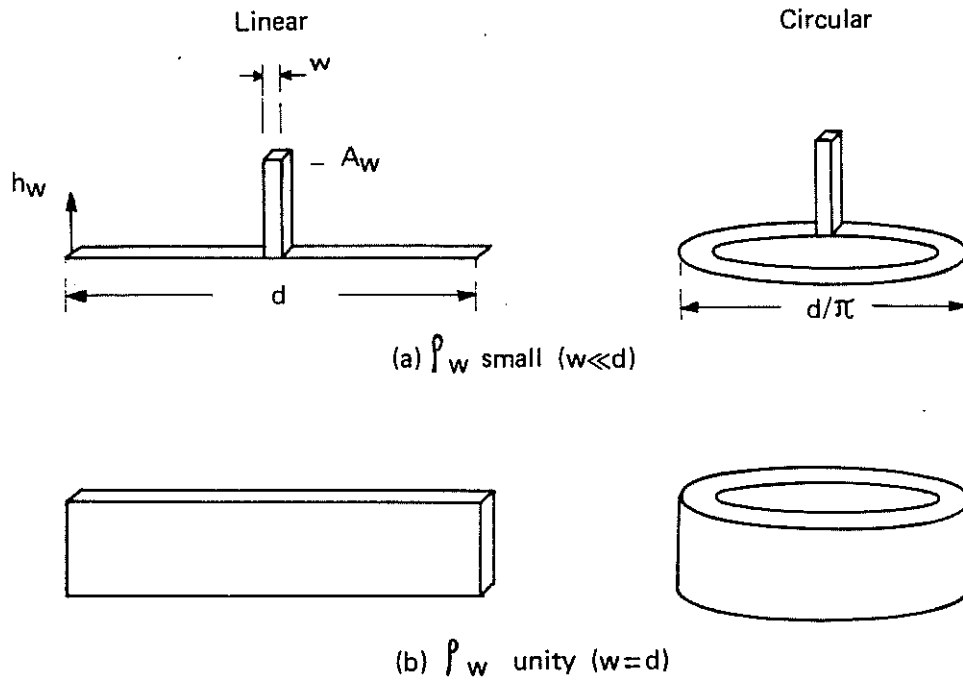
Fig. 5_ UNSTEADY AND STEADY DISTURBANCE–LINEAR AND
CIRCULAR SOURCE REGION

(a) blade displacement distribution

(b) blade force distribution
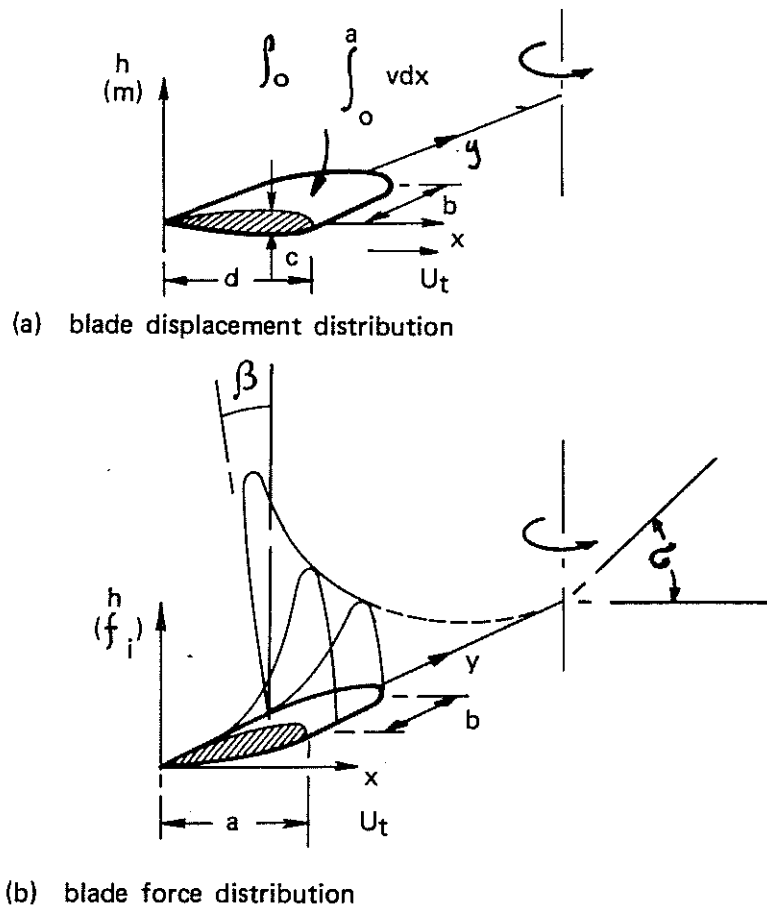
Fig. 6   BLADE DISPLACEMENT AND FORCE DISTRIBUTIONS
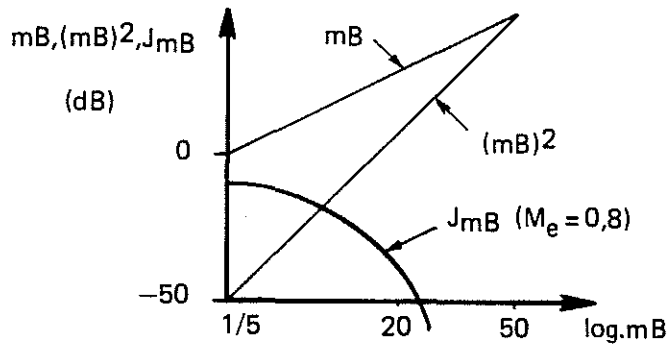
(a) Individual radiation terms
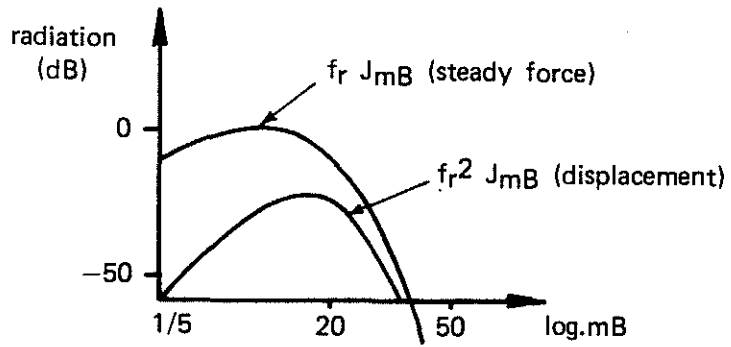
(b) Resultant spectrum

Fig. 7- COMPARISON BETWEEN STEADY FORCE AND
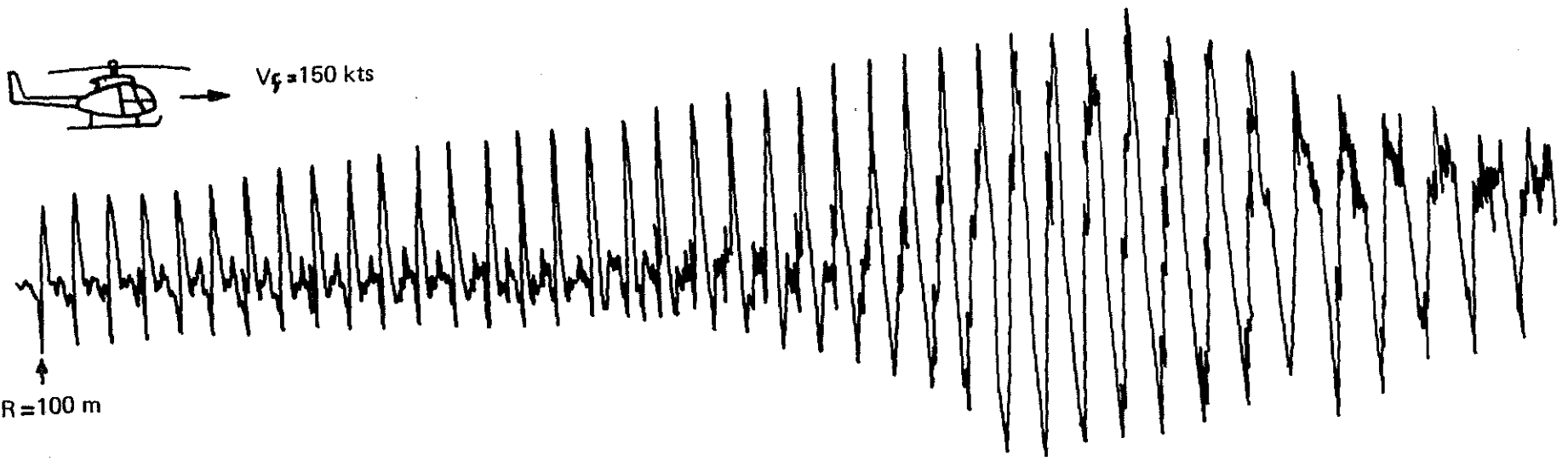DISPLACEMENT RADIATION
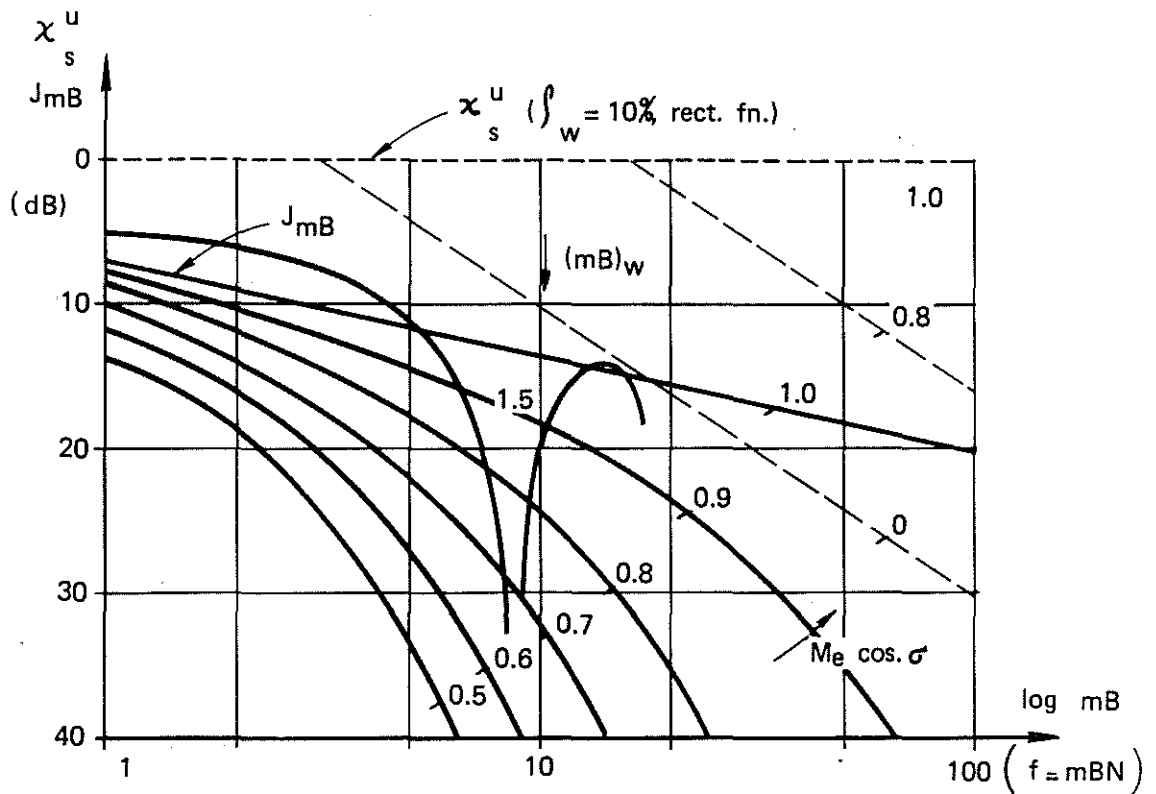
Fig. 8 - COMPARISON BETWEEN UNSTEADY (χ^u_s)

AND STEADY (J_{mB}) SPECTRUM FUNCTIONS

$V_f \approx 150$ kts

overhead

R = 100 m

∫ P dt

T/4   T/2   t

P

T rotational period

(c) R ≈ 100m

L

−90   90   180   270   θ

$\dfrac{\partial L}{\partial \theta}$

θ
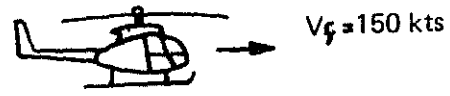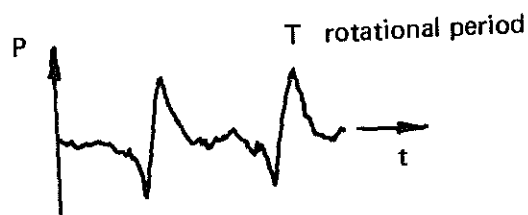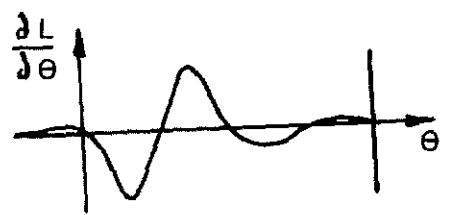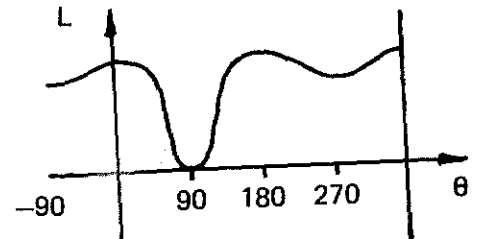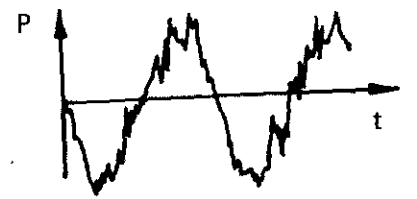
(a) Typical disc loading. $r_e \approx 0.9\, r_t$

∫ P dt

T/4   T/2   t

P

t
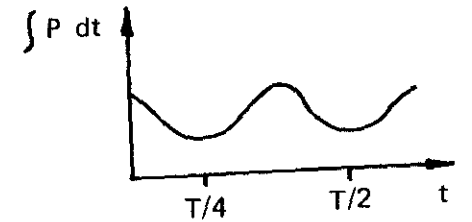
(b) Overhead

Fig.9 HIGH SPEED FLIGHT ACOUSTIC SIGNATURE PUMA SA. 330